J Mater Sci (2006) 41:5851–5856
DOI 10.1007/s10853-006-0324-0

Morphology and modulus of vapor grown carbon nano fibers

Tetsuya Uchida · David P. Anderson · Marilyn L. Minus · Satish Kumar

Received: 11 May 2004 / Accepted: 28 July 2005 / Published online: 28 June 2006

Abstract Two types of morphologies have been observed in vapor grown carbon nano fibers (CNFs) using transmission electron microscopy (TEM). In one case, a truncated cone microstructure was observed, with outer and inner diameters of 60 and 25 nm, respectively. In this type of CNF, graphite sheets were oriented at about 15° to the fiber axis. The second type of fiber was a double-layer CNF with outer and inner diameters of 83 and 20 nm, respectively. A truncated cone structure was also observed in the double-layer CNF. Graphite sheets in the outer layer of the double-layer fibers were oriented along the nano fiber axis. Tensile modulus for the first type of nano fiber along its axis was calculated to be 50 GPa, and for the second type of fiber the calculated modulus value was in the 100–775 GPa range, depending on the outer layer orientation. Modulus calculations based on these two morphologies explain the wide ranging experimental CNF modulus values reported in the literature.

T. Uchida
Graduate School of Natural Science and Technology, Okayama University, Okayama 700-8530, Japan

M. L. Minus · S. Kumar (✉)
School of Polymer, Textile and Fiber Engineering, Georgia Institute of Technology, Atlanta, Georgia 30332-0295, USA
e-mail: satish.kumar@ptfe.gatech.edu

D. P. Anderson
University of Dayton Research Institute, Dayton, OH 45469-0168, USA

Present address: T. Uchida
Faculty of Engineering, Okayama University, Okayama 700-8530, Japan

Introduction

Carbon fibers (typical diameter 7–10 μm) for reinforcing composites were developed during the 1960s, while the development of carbon nano fibers (CNFs, typical outer diameter 50–200 nm) dates to the 1980s [1–4]. Reports of vapor grown carbon fibers prior to 1980 also exist [5–7]. The existence of carbon nanotubes was recognized in 1991 [8], which are now being produced with multi-walls, double walls or a single wall, and are considered to be the ultimate reinforcing systems [9]. While carbon fibers have been used for reinforcing composites over the last four decades, there is significant current research activity for making macroscopic fibers from CNFs [10–14], multiwall carbon nanotubes [15, 16] and single wall carbon nanotubes [17–20]. Thermal [21] and electrical conductivity [22] as well as mechanical properties [4, 23] of the CNFs have been reported. Property improvements in the polymeric fibers with the incorporation of CNFs include enhanced tensile modulus [10, 12], torsional modulus [11], compressive strength [11] and reduced thermal shrinkage [12]. Carbon nano fibers are also being used to reinforce functional materials [24].

Vapor grown CNFs are grown by exposing a metallic catalyst to hydrocarbon gases [25]. Based on high resolution transmission electron microscopy (TEM) studies of the vapor grown CNF produced by the Floating Reactant Method, cup-stacked-type structures with entirely hollow cores have been reported [26, 27]. The graphite sheets were not parallel to the fiber axis, though the sheet angle was not quantified. For fully understanding the mechanical properties (particularly the modulus) of this type of CNF, the orientation of the graphite sheets is important, as the graphite modulus drops significantly with orientation [28]. A similar drop in modulus with orientation has also been reported in single wall carbon nanotube bundles of relatively large diameter [29].

CNF modulus of 680 GPa [30], 100–210 GPa [31], and 130–250 GPa [32] has been reported. Recent studies on the composite fibers suggest that the CNF modulus may be below 100 GPa [10, 14]. In this paper, we discuss the morphology and modulus of the vapor grown CNFs.

Experimental

Carbon nano fibers (PR-24-HT, PR-24-PS, PR-21-PS) were obtained from Applied Sciences Inc., Cedarville, Ohio [1]. For TEM study, CNFs (PR-24-HT) were dispersed in ethanol by sonication, and a drop of this suspension was placed on a lacey carbon grid and dried in air at room temperature. TEM studies were carried-out on a JEOL 4000EX microscope at 400 kV and the images were recorded on Kodak SO-163 film. For X-ray studies, nickel filtered CuKα radiation (wavelength = 0.15418 nm) was used with a Statton flat-film camera equipped with an image plate. The intensities at the Bragg angle of the graphitic (002) peak were measured as a function of azimuthal angle relative to the fiber equatorial direction in poly(methyl methacrylate) (PMMA)/CNF composite fiber. Processing and properties of PMMA/CNF composite fibers have been reported [12].

Results and discussion

Single and double layer morphologies were observed in the PR-24-HT fiber. The number and weight average length of the PR-24-HT fiber determined from TEM images were 2 and 8 μm, respectively. Figure 1 shows the single layer CNF. The outer and inner radii of the single layer CNF were ~30 and 12.5 nm, respectively. The inner and outer walls were oriented at ~15–17° to the fiber axis (Fig. 1b, c). These morphological features appear to arise from the CNF growth mechanism [33], and suggest that graphite sheets orient at this angle. High resolution electron micrographs of this type of CNF (Fig. 2) confirmed that the graphite sheets were oriented parallel to each other and at an average angle of ~15° to the nano fiber axis. The crystallite thickness perpendicular to the graphitic planes was ~17 nm (Fig. 2).

The PMMA/CNF [12] composite fiber exhibited a four point X-ray diffraction corresponding to the graphite (002) peak (Fig. 3). The azimuthal intensity data in Fig. 3 was fitted with two Gaussian peaks of the same widths symmetrically placed about the equator. The parameters, full-width at half-maximum (FWHM) and peak separation half-angle (or the angle from the equator) reported in Table 1 are also shown in Fig. 3. The FWHM of the azimuthal scan is a measure of the spread of orientation of the graphene planes within the PMMA/CNF composite fiber, which can result from variation in graphite plane orientation within a nano fiber as well as from the variation in nano fiber orientation in the composite fiber. The peak separation angle is related to the average graphene plane orientation angle by the following equation [34]:

$$\cos\beta = \frac{\cos\phi}{\cos\theta} \tag{1}$$

where, θ is the diffraction angle ($2\theta = 26.5°$ for the graphite (002) plane), and ϕ is the compliment of the angle that the graphene plane makes with the fiber axis, while β is the compliment of the peak separation half-angle. Based on the X-ray studies of the composite fiber, the average graphite plane orientation with respect to the nano fiber axis was determined to be 11.8° for PR-21-PS and 13.1° for PR-24-PS fibers. Similarly graphene plane misorientation angle in the range of 14–17° was determined from X-ray diffraction studies on poly(ethylene terephthalate) (PET)/CNF composite fibers. Using the radial scan of the PMMA/CNF composite fiber diffraction pattern, graphite crystal size perpendicular to (002) plane as determined using the Scherrer equation was 16 nm for the PR-24-PS fiber, comparable to the value of 17 nm determined from the high resolution TEM on the heat-treated fiber (PR-24-HT).

The high resolution electron micrograph in Fig. 2 shows that 3–5 graphite sheets were folded together. Folding was observed at both inner and outer surface of the wall, and the diameter of the fold is about one nanometer. Some of the graphite layers were folded several times. The folding morphology of the graphite sheet may affect the mechanical properties of the CNFs. The length between the two folds was about 60 nm. The nano fiber morphologies are schematically shown in Fig. 4.

The TEM of the double layer CNF with inner and outer radii of 10 and 41.5 nm, respectively, is given in Fig. 5. In the double layer CNF, the angle of the inner graphite sheets was not constant, and varied between 4 and 36° (Fig. 6). In addition, some closed graphite sheets were also observed in the hollow core region (see arrow in Figs. 5 and 6). The outer layer in the double layer CNF was oriented along the nano fiber axis as shown schematically in Fig. 4b. The double-layer structure was also reported by Endo et al. [26]. However, in their case amorphous carbon appears to cover the truncated inner layer structure, while the clear graphitic layers can be seen in Fig. 6. Amorphous carbon was also occasionally observed on the CNF surface in this study.

Carbon nano fiber modulus was calculated using continuum mechanics. If θ_{graphite} is the angle between graphite sheets and the fiber axis, then the modulus along the fiber axis, $\langle E \rangle$, is given by the following equation [29].

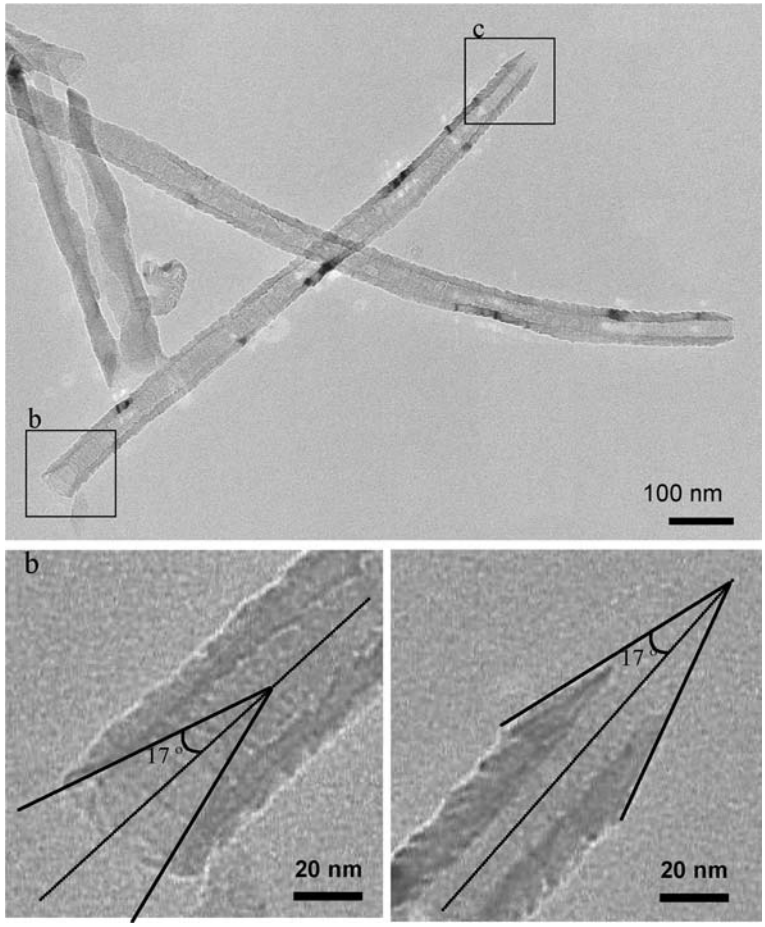

Fig. 1 Transmission electron micrographs of the single-layer carbon nano fibers

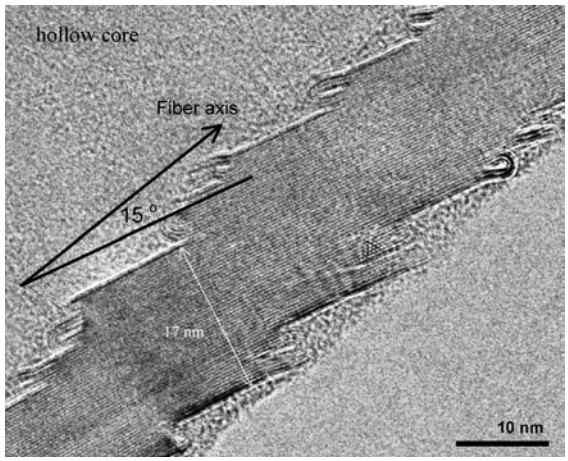

Fig. 2 High resolution transmission electron micrograph of the single-layer carbon nano fiber

$$\frac{1}{\langle E\rangle} = \frac{1}{E_2} + \left(\frac{1}{G_{12}} - \frac{2\upsilon_{12}}{E_1} - \frac{2}{E_2}\right)\langle \cos^2\theta_{\text{graphite}}\rangle + \left(\frac{1}{E_1} + \frac{1}{E_2} - \frac{1}{G_{12}} + \frac{2\upsilon_{12}}{E_1}\right)\langle \cos^4\theta_{\text{graphite}}\rangle \quad (2)$$

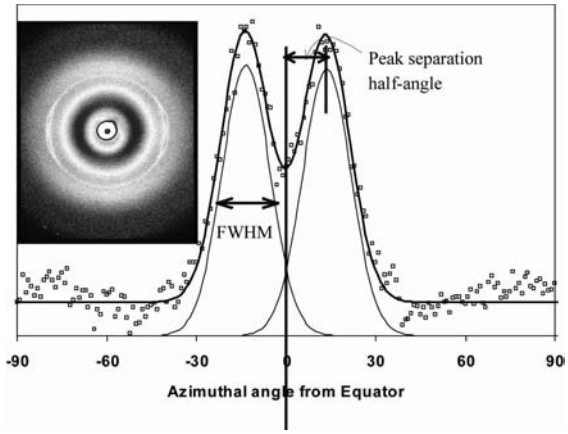

Fig. 3 Azimuthal scan of the graphitic (002) X-ray diffraction for CNF (PR-24-PS) in PMMA/CNF composite fiber and a flat plate photograph (inset)

where, E_1, E_2, and G_{12} and are longitudinal, transverse, and in-plane shear moduli, respectively, and v_{12} is the Poisson's ratio (Table 2). Carbon nano fibers have hollow cores, and based on the geometric considerations, the effective modulus (E_{eff}) of the single and double layer CNFs is calculated using Eqs. 3 and 4, respectively:

Table 1 X-ray diffraction orientation results

Sample	FWHM	Peak separation half-angle (90-β) (°)	Average graphite plane angle with respect to the fiber axis (90-ϕ) (°)	Effective modulus (Calculated using Eqs. 2 and 3) (GPa)
PMMA/PR-21-PS fiber	19.2	12.1	11.8	76
PMMA/PR-24-PS fiber	19.0	13.5	13.1	63

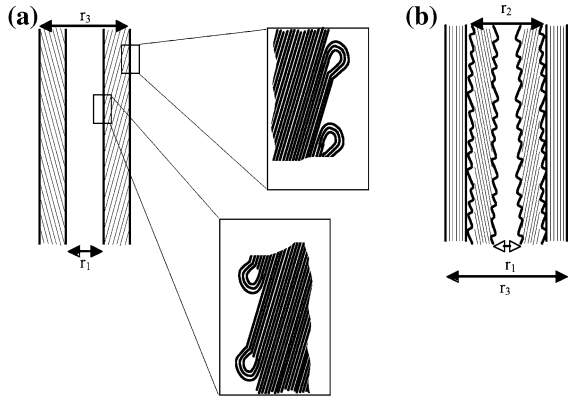

Fig. 4 Schematic illustrations of (**a**) single-layer carbon nano fiber, (**b**) double-layer carbon nano fiber

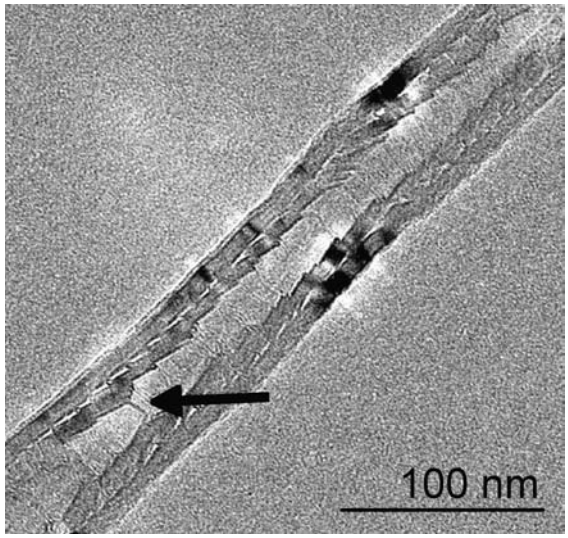

Fig. 5 Transmission electron micrograph of the double-layer carbon nano fiber

$$E_{\text{eff}} = E\left(\frac{r_3^2 - r_1^2}{r_3^2}\right) \tag{3}$$

$$E_{\text{eff}} = E_{\text{inner}}\left(\frac{r_2^2 - r_1^2}{r_3^2}\right) + E_{\text{outer}}\left(\frac{r_3^2 - r_2^2}{r_3^2}\right) \tag{4}$$

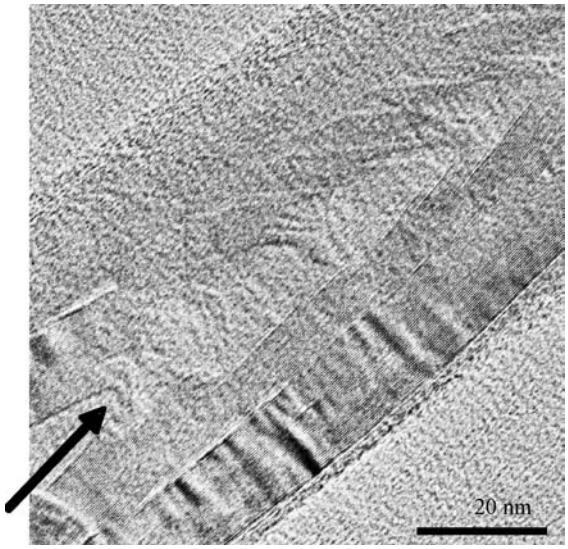

Fig. 6 High resolution transmission electron micrograph of the double-layer carbon nano fiber

where r_1, r_2, and r_3 have been defined in Fig. 4. E is the single layer CNF modulus calculated from Eq. 2, based on the graphite plane misorientation. For the double layer CNF, this modulus calculated from Eq. 2 for the inner layer has been termed as E_{inner}. The modulus of the outer layer of the double layer CNF is E_{outer}. The misorientation angle for the outer layer is less than 10°. Based on Eq. 2, the outer layer modulus can range between 120 and 1060 GPa for the orientation range of 0–10° [28].

Using Eqs. 2 and 3, the effective axial modulus of the single layer CNF (PR-24-HT) was calculated to be 50 GPa for a 15° graphite plane misorientation. Similarly moduli values of 63 and 76 GPa were calculated for PR-24-PS and PR-21-PS nano fibers based on their respective graphite plane misorientation angles of 13.1 and 11.8°. For comparison, CNF moduli were estimated to be in the 22–100 GPa range based on the experimental data from PEEK/CNF, PP/CNF and PMMA/CNF composite fibers [10, 12, 14]. The upper and lower limits of the effective axial modulus for the double layer CNF were calculated to be 775 and 100 GPa based on the outer layer misorientation of 0 and 10°, respectively, where the average misorientation angle for the inner layer was fixed at 15°. Figure 7

Table 2 Graphite elastic constants and carbon nano fiber (PR-24-HT) parameters

E_1	1060 GPa
E_2	36.5 GPa
G_{12}	4 GPa
υ_{12}	0.3
θ (CNF)	15°
r_3 (CNF)—single layer	30 nm
r_1 (CNF)—single layer	12.5 nm
E_{eff} (CNF)—single layer	50 Gpa
r_3 (CNF)—double layer	41.5 nm
r_2 (CNF)—double layer	22 nm
r_1 (CNF)—double layer	10 nm

shows the effective modulus for the double layer CNF as a function of the outer layer misorientation. CNF modulus estimated from the composites data should account for morphological changes in the polymer resulting from the presence of CNFs. If the presence of CNFs results in changes in polymer crystallinity and/or orientation, and if these changes are not accounted for, then the CNF modulus determined from such experimental data will be in error. The CNF modulus of 22 GPa is an underestimate for these reasons [14]. Due to graphite sheet folding (Figs. 2, 4), the in-plane shear modulus is likely to be higher than the value used (4 GPa) for the individual unconnected graphite layer stackings. The calculated value of 50 GPa is thus the lower limit for the modulus of PR-24-HT CNF. The calculated values were based on the graphite elastic constants. Due to the high temperature (above 2800°C in inert environment) heat-treatment, the structure of PR-24-HT is highly graphitic. On the other hand the structure of PR-24-PS and PR-21-PS is likely to be less graphitic, and may contain significant turbostratic graphite. For example, if the outer layer of the double layer CNF is turbostratic graphite with an axial modulus (E_{outer}) of 237 GPa [4], then the modulus of the double layer CNF using Eq. 4 is calculated to be

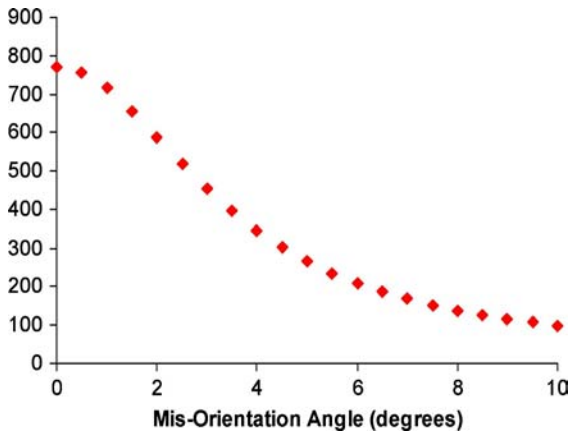

Fig. 7 Effective modulus of the double layer carbon nano fiber as a function of misorientation of the graphite planes in the outer layer. Orientation of the inner layer is fixed at 15° with respect to the fiber axis

180 GPa. These calculations explain the wide ranging CNF moduli values reported in the literature [4, 10, 14, 30–32].

Conclusions

Single and double layer morphologies have been observed in the vapor grown CNFs. In the single-layer CNFs, graphite sheets are oriented at ~15° to the fiber axis. A lower limit for the axial modulus of this fiber was calculated to be 50 GPa. On the other hand, in the double-layer CNF, the graphite sheets in the outer layer exhibit an orientation of less than 10°. The calculated axial moduli based on the graphite elastic constants are 775 and 110 GPa for the outer layer orientation of 0 and 10°, respectively. If the outer layer is turbostratic graphite, then the modulus of the double layer fiber is calculated to be 180 GPa. The CNF modulus has a strong dependence on the graphite plane misorientation. The CNF morphological observations reported here along with the modulus calculations explain the wide ranging CNF modulus values reported in the literature.

Acknowledgements Partial support for this work from National Science Foundation, Air Force Office of Scientific Research (F49620-03-1-0124) and by the United States Air Force Research Laboratory at Wright-Patterson Air Force Base, OH (contract F33615-00-D-5006) is gratefully acknowledged.

References

1. Tibbetts GG, Devour MG (1986) U.S. patent 4,565,684
2. Lake ML, Ting JM (1999) In: Burchell TD (ed) Carbon materials for advanced technologies. Oxford, UK, p 139
3. De Jong KP, Geus JW (2000) Catal Rev Sci Eng 42:481
4. Tibbetts GG, Beetz CP Jr (1987) J Phys D Appl Phys 20:292
5. Gibson J, Riley HL, Taylor J (1944) Nature 154:544
6. Koyama T (1972) Carbon 10:757
7. Chemical Engineering, October (1957) 172–174
8. Iijima S (1991) Nature 354:56
9. Lau KT, Chipara M, Ling HY, Hui D (2004) Composites Part B 35:95
10. Kumar S, Doshi H, Srinivasarao M, Park JO (2002) Polymer 43:1701
11. Ma H, Zeng J, Realff ML, Kumar S, Schiraldi DA (2003) Comp Sci Tech 63:1617
12. Zeng J, Saltysiak B, Johnson WS, Schiraldi AD, Kumar S (2004) Composites Part B 35:173
13. Uchida T, Dang TD, Min BG, Zhang X, Kumar S (2005) Composites Part B 36:183
14. Sandler J, Windle AH, Werner P, Altatädt V, Es MV, Shaffer MSP (2003) J Mater Sci 38:2135
15. Li YL, Kinloch IA, Windle AH (2004) Science 304:276
16. Zhang M, Atkinson KR, Baughman RH (2004) Science 306:1358
17. Ericson LM, Fan H, Peng H, Davis VA, Zhou W, Sulpizio J, Wang Y, Booker R, Vavro J, Guthy C, Parra-Vasquez ANG, Kim MJ, Ramesh S, Saini RK, Kittrell C, Lavin G, Schmidt H, Adams WW, Billups WE, Pasquali M, Hwang WF, Hauge RH, Fischer JE, Smalley RE (2004) Science 305:1447

18. Kumar S, Dang TD, Arnold FE, Bhattacharayya AR, Min BG, Zhang X, Vaia RA, Park C, Adams WW, Hauge RH, Smalley RE, Ramesh S, Willis PA (2002) Macromolecules 35:9039
19. Sreekumar TV, Liu T, Min BG, Guo H, Kumar S, Hauge RH, Smalley RE (2004) Adv Mater 16:58
20. Chae HG, Sreekumar TV, Uchida T, Kumar S (2005) Polymer 46:10925
21. Heremans J, Beetz CP Jr (1985) Phys Rev B 32:1981
22. Heremans J (1985) Carbon 23:431
23. Endo M, Kim YA, Hayashi T, Nishmura K, Matusita T, Miyashita K, Dresselhaus MS (2001) Carbon 39:1287
24. Koerner H, Price G, Pearce NA, Alexander M, Vaia RA (2004) Nat Mater 3:115
25. Tibbetts GG (1989) Carbon 27:745
26. Endo M, Kim YA, Hayashi T, Fukai Y, Oshida K, Terrones M, Yanagisawa T, Higashi S, Dresselhaus MS (2002) Appl Phys Lett 80:1267
27. Endo M, Kim YA, Hayashi T, Yanagisawa T, Muramatsu H, Ezaka M, Terrones H, Terrones M, Dresselhaus MS (2003) Carbon 41:1941
28. Watt W, Perov BV (1985) In: Handbook of composites: strong fibers, vol 1. Elsevier, Amsterdam, p 392
29. Liu T, Kumar S (2003) Nano Lett 3(5):647
30. Jacobsen RL, Tritt TM, Guth JR, Ehrlich AC, Gillespie DJ (1995) Carbon 33:1217
31. Ting J (1999) J Mater Sci 34:229
32. Ishioka M, Okada T, Matsubara K (1992) J Mater Res 7:3019
33. Terrones H, Hayashi T, Munoz_Navia M, Terrones M, Kim YA, Grobert N, Kamalakaran R, Dorantes-Davia J, Escudero R, Dresselhaus MS, Endo M (2001) Chem Phys Lett 343:241
34. Alexander LE (1969) In: X-ray diffraction methods in polymer science. Wiley-Interscience, John Wiley & Sons, Inc., New York